

# Alkali-Metal Salts of Aromatic Carboxylic Acids: Liquid Crystals without Flexible Chains

Rik Van Deun,<sup>[a]</sup> Jan Ramaekers,<sup>[a]</sup> Peter Nockemann,<sup>[a]</sup> Kristof Van Hecke,<sup>[a]</sup>  
Luc Van Meervelt,<sup>[a]</sup> and Koen Binnemans<sup>\*[a]</sup>

**Keywords:** Alkali metals / Layered compounds / Liquid crystals / Metallomesogens / Smectic mesophases

The alkali-metal salts of *meta*-substituted benzoic acids exhibit a smectic A mesophase at high temperatures. These compounds are examples of liquid crystals without terminal alkyl chains. The influence of the metal ion and of the type of substituents on the transition temperatures is discussed. Compounds with the substituent in the *ortho*- and *para*-positions are non-mesomorphic. The crystal structures of the

compounds  $\text{Rb}(\text{C}_7\text{H}_4\text{ClO}_2)(\text{C}_7\text{H}_4\text{ClO}_2\text{H})$ ,  $\text{Na}(\text{C}_7\text{H}_4\text{IO}_2)(\text{H}_2\text{O})$ ,  $\text{K}(\text{C}_7\text{H}_4\text{ClO}_2)(\text{C}_7\text{H}_4\text{ClO}_2\text{H})$  and  $\text{Rb}(\text{C}_7\text{H}_4\text{BrO}_2)(\text{C}_7\text{H}_4\text{BrO}_2\text{H})$  have been determined by X-ray crystallography. These compounds possess a layerlike structure in the solid state.

(© Wiley-VCH Verlag GmbH & Co. KGaA, 69451 Weinheim, Germany, 2005)

## 1 Introduction

In the classic picture, liquid crystals are either calamitic (rodlike) or discotic (disklike) molecules. However, many types of liquid crystals cannot be classified as rodlike or disklike, and several intermediate forms are possible.<sup>[1,2]</sup> In general, the rodlike mesogenic molecules have one or two terminal alkyl chains. The function of these flexible chains is not only to stabilize the mesophase, but also to reduce the melting point. This may give the wrong impression that such flexible chains are necessary to obtain liquid crystals, as some compounds without a flexible chain are able to form a mesophase as well. Typical examples are the *para*-oligophenyls, such as *para*-quinquephenyl and *para*-sexiphenyl.<sup>[3–6]</sup> Tschierske and co-workers<sup>[7]</sup> have investigated semi-rigid substituted benzyloxybiphenyl compounds with diol head groups. The indenenes and pseudo-azulenes with peripheral chloro groups reported by Barbera et al.<sup>[8]</sup> were the first examples of mesomorphic discotic molecules without a flexible chain. The rodlike or disklike shape of all these molecules is very distinct. We can therefore ask ourselves what happens if the length of the rodlike molecules is reduced. Do simple aromatic compounds consisting of one phenyl ring exhibit a mesophase? The answer is no; compounds such as benzoic acid, phenol, aniline, chlorobenzene are not liquid crystals. However, the situation changes when alkali-metal salts of aromatic carboxylic acids (for example sodium benzoate) are considered. The liquid-crystalline behaviour of these compounds was discovered in 1910 by the great pioneer in liquid-crystal research,

Daniel Vorländer.<sup>[9,10]</sup> Vorländer investigated the lithium, sodium, potassium and rubidium salts of benzoic acid. In addition, he investigated the alkali-metal salts of the *ortho*-, *meta*- and *para*-isomers of chlorobenzoic acid, bromobenzoic acid, iodobenzoic acid, methylbenzoic acid and nitrobenzoic acids. The sodium and potassium salts were prepared for all these compounds and a few lithium, rubidium and cesium salts as well. Vorländer mentions only the presence and absence of a mesophase, but gives no mesophase identification. These mesophases often have a low viscosity, and approximate transition temperatures were given for a limited number of compounds only. Demus and co-workers<sup>[11]</sup> re-examined some of the compounds described by Vorländer — the lithium, sodium, potassium, rubidium and cesium salts of 3-bromobenzoic acid, and the potassium salt of 3-iodobenzoic acid — in 1970. In some instances they used the original samples prepared by Vorländer sixty years before, and they found no signs of deterioration. These authors determined the transition temperatures by optical microscopy and identified the mesophase as a “neat” phase (smectic A). In addition, they constructed binary phase-diagrams by mixing the compounds with other aliphatic and aromatic carboxylate salts. Unfortunately, there is not complete agreement between the results of Vorländer and Demus: transition temperatures for the same compound reported by the two authors differ by up to 35 °C in some cases, and for cesium 3-bromobenzoate Vorländer found a mesophase, whereas Demus and co-workers didn't.

Given the intrinsic scientific interest of these low-molecular-weight liquid crystals, we reinvestigated the compounds described by Vorländer in order to obtain more detailed quantitative thermodynamic and structural data. The com-

<sup>[a]</sup> Katholieke Universiteit Leuven, Department of Chemistry  
Celestijnenlaan 200F, 3001 Leuven, Belgium  
Fax: + 32-16-327-992  
E-mail: Koen.Binnemans@chem.kuleuven.ac.be

pounds were investigated by polarizing optical microscopy (POM) and by differential scanning calorimetry (DSC), and some compounds by high-temperature X-ray diffraction. This work extends Vorländer's work by including some alkali-metal salts of substituted benzoic acids not studied by Vorländer, for instance salts of the *ortho*-, *meta*- and *para*-isomers of fluorobenzoic acid and methoxybenzoic acid. In addition, we have determined the crystal structures of four alkali-metal salts.

## Results and Discussion

The first series of compounds we prepared were the alkali-metal salts of benzoic acid. These compounds have much higher transition temperatures than benzoic acid, which melts at 122 °C. The melting points of the corresponding alkali-metal salts range from 369 °C (lithium benzoate) to 444 °C (rubidium benzoate). While benzoic acid does not exhibit liquid-crystalline behaviour, sodium benzoate is an enantiotropic liquid crystal. The other salts (the lithium, potassium, rubidium and cesium benzoates) do not exhibit mesomorphism. The optical texture of the sodium benzoate shows the typical features of a smectic A phase (SmA): bâtonnets appear from the isotropic liquid and coalesce to a fan-shaped texture with homeotropic regions. If the sample is quickly cooled after isotropisation, thermal decomposition can be limited and formation of a mesophase can be observed upon cooling, thus illustrating the enantiotropic nature of the SmA mesophase. The DSC thermogram (first heating run) of sodium benzoate is shown in Figure 1. The thermal behaviour of the alkali-metal benzoates is summarised in Table 1.

Table 1. Thermal behaviour of benzoic acid and its alkali-metal salts

Compound	Transition temperatures (°C) <sup>[a]</sup>
Benzoic acid	Cr·122·I
Lithium benzoate	Cr·369·I
Sodium benzoate	Cr·431·SmA·451·I
Potassium benzoate	Cr·439·I
Rubidium benzoate	Cr·444·I
Cesium benzoate	Cr·383·Cr <sub>II</sub> ·398·I

<sup>[a]</sup> Cr, Cr<sub>I</sub>, Cr<sub>II</sub>: solid crystalline phases; SmA: smectic A phase; I: isotropic phase.

These findings are in partial disagreement with the data of Vorländer, who reported that the lithium, sodium, potassium and rubidium salts of benzoic acid are all enantiotropic liquid crystals, while benzoic acid is not liquid-crystalline. He described the texture as small rods which flow together to form drops. The transition temperatures of sodium benzoate were given (melting point: 410 °C, clearing point: 430 °C), but not for the other unsubstituted alkali-metal benzoates. Vorländer had problems to record the transition temperatures of these high-melting solids accurately due to their thermal decomposition at high temperatures. For rubidium benzoate, Vorländer wrote that this

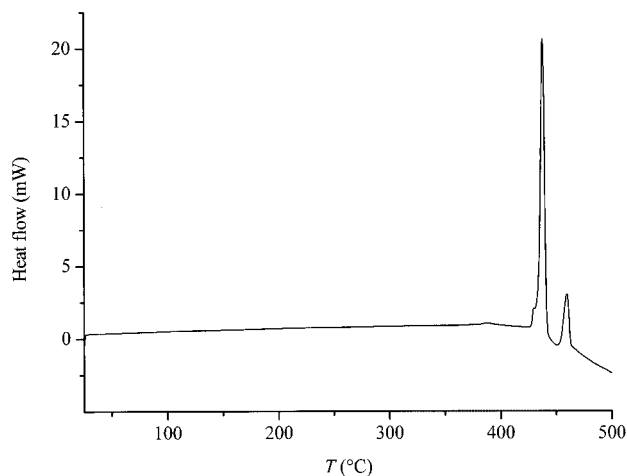


Figure 1. DSC thermogram (first heating) of sodium benzoate; endothermic peaks are pointing upwards

compound decomposed before the clearing point had been reached. Modern techniques indicate that only the sodium salt is a liquid crystal, and the other salts of benzoic acid melt to an isotropic liquid without showing a mesophase, just like benzoic acid itself. No evidence for monotropic mesophases was found.

A second group of compounds we investigated are the sodium salts of different *meta* (or 3)-substituted benzoic acids: sodium 3-fluorobenzoate, sodium 3-chlorobenzoate, sodium 3-bromobenzoate, sodium 3-iodobenzoate, sodium 3-methylbenzoate and sodium 3-methoxybenzoate (Figure 2). Their thermal behaviour was compared to that of unsubstituted sodium benzoate; the data are summarised in Table 2. As can be seen, all *meta*-substituted sodium benzoates are

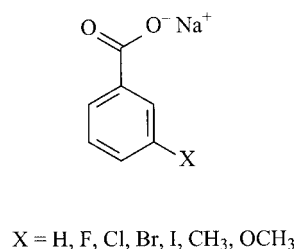


Figure 2. Structures of sodium salts of *meta*-substituted benzoic acids

Table 2. Thermal behaviour of *meta*-substituted sodium benzoates

Compound	Transition temperatures (°C) <sup>[a]</sup>
Sodium benzoate	Cr·431·SmA·451·I
Sodium 3-fluorobenzoate	Cr·406·SmA·415·I
Sodium 3-chlorobenzoate	Cr·337·SmA·408·I
Sodium 3-bromobenzoate	Cr·306·SmA·389·I
Sodium 3-iodobenzoate	Cr·278·SmA·372·I
Sodium 3-methylbenzoate	Cr·333·SmA·384·I
Sodium 3-methoxybenzoate	Cr·275·SmA·291·I

<sup>[a]</sup> Cr: solid crystalline phase; SmA: smectic A phase; I: isotropic phase.

enantiotropic liquid crystals. For the *meta*-halogen-substituted compounds, the melting points decrease with increasing size of the halogen substituent in the *meta*-position, as is also the case for the clearing points (Figure 3). However, the melting points decrease in a more pronounced way than the clearing points, which results in an increase of the mesophase range.

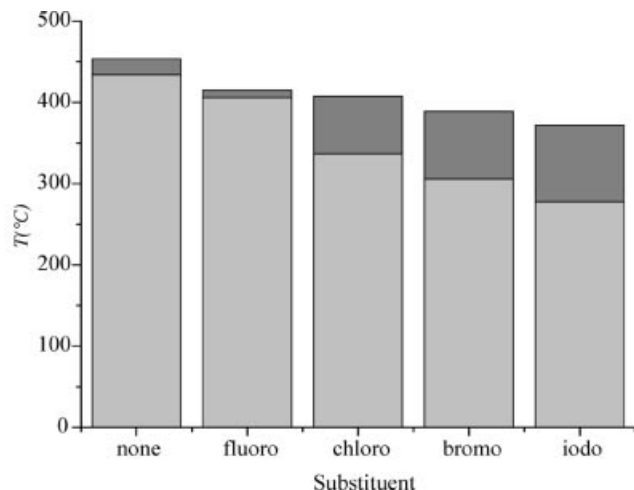


Figure 3. Influence of the size of the halogen atom on the transition temperatures of the sodium salts of *meta*-halogen-substituted benzoic acids; the light-grey shading represents the solid state and the dark-grey shading the smectic A phase

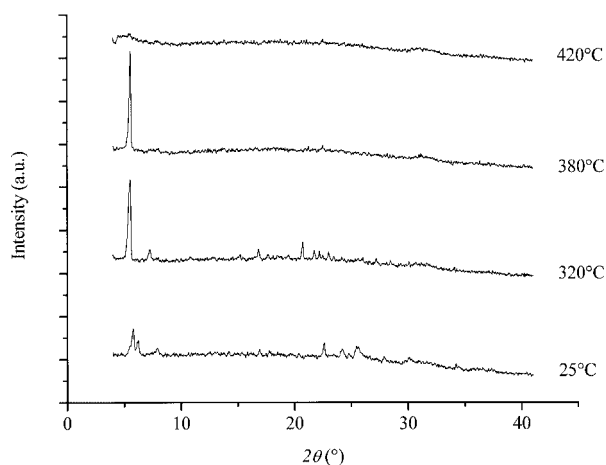


Figure 4. X-ray diffractograms of sodium 3-chlorobenzoate recorded at different temperatures

Figure 4 shows the X-ray diffractograms of sodium 3-chlorobenzoate. The bottom trace is that of a powder diffractogram at room temperature. At small diffraction angles, the diffraction peaks indicate a rather long-distance ordering, while the peaks at wider diffraction angles (around  $2\theta = 25^\circ$ ) result from an ordering at low dimensions. The observation of a number of diffraction peaks in the X-ray diffractogram confirms the crystallinity of the compound at room temperature. The second-from-bottom trace shows the compound after heating to 320 °C. The

compound is still in the solid state, but evidence of a layered structure is already given by the first-order diffraction peak at around  $2\theta = 6^\circ$ , which is of a rather high intensity. The third trace shows the situation at 380 °C, where the compound is in the SmA mesophase. Only the long-range order of the layered smectic phase remains, as witnessed by the absence of all but the first-order peak in the diffractogram. This is a typical diffractogram of a disordered smectic phase. The upper trace is of the sample in the isotropic liquid. No order remains, as can be seen from the absence of sharp diffraction peaks. The identification of the mesophase was supported by the observation of the texture given in Figure 5, which shows the formation of bâtonnets, which is typical for a smectic A phase. The thermal stability of the compounds at high temperatures is limited, as can be seen from the DSC curve of sodium 3-chlorobenzoate shown in Figure 6. Although the melting and clearing peaks are

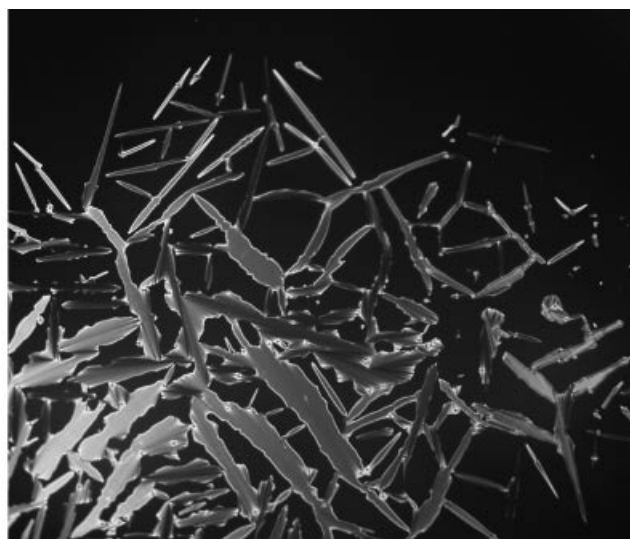


Figure 5. Texture of sodium 3-bromobenzoate at the clearing point at 389 °C, after cooling down from the isotropic liquid

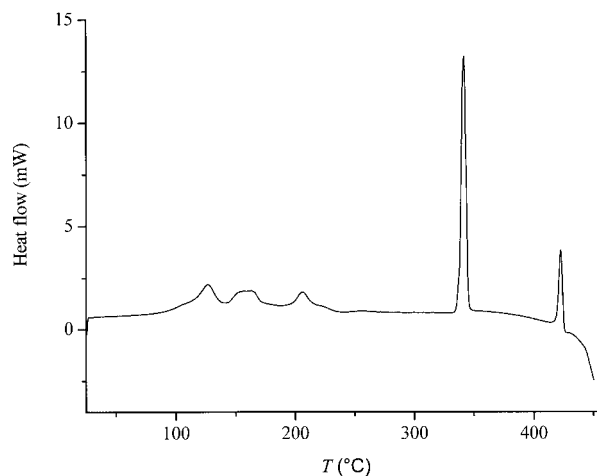


Figure 6. DSC thermogram of sodium 3-chlorobenzoate (first heating); endothermic peaks are pointing upward; the transitions between 100 and 250 °C are crystal–crystal transitions

sharp, which indicates a high purity, decomposition of the sample occurs already at temperatures below 400 °C.

The potassium salts of *meta*-substituted benzoic acids form a third group of compounds. The general trends observed for the sodium salts remain the same for the potassium salts: the melting and clearing temperatures decrease with increasing size of the *meta*-halogen substituent, whereas the mesophase range increases in the same way. However, unsubstituted potassium benzoate does not show a mesophase (see discussion of unsubstituted alkali-metal benzoates and Table 1), and neither does potassium 3-fluorobenzoate. Generally speaking, the transition temperatures of the potassium salts are lower than those of the corresponding sodium salts, and the mesophase range for an analogous potassium salt is narrower than that of the comparable sodium salt. The thermal behaviour of the potassium *meta*-substituted benzoates is summarised in Table 3.

Table 3. Thermal behaviour of *meta*-substituted potassium benzoates

Compound	Transition temperatures (°C) <sup>[a]</sup>
Potassium benzoate	Cr·439·I
Potassium 3-fluorobenzoate	Cr·407·I
Potassium 3-chlorobenzoate	Cr·316·SmA·377·I
Potassium 3-bromobenzoate	Cr·292·SmA·367·I
Potassium 3-iodobenzoate	Cr·265·SmA·357·I
Potassium 3-methylbenzoate	Cr·295·SmA·406·I
Potassium 3-methoxybenzoate	Cr·261·SmA·301·I

<sup>[a]</sup> Cr: solid crystalline phase; SmA: smectic A phase; I: isotropic phase.

The fourth and fifth group, consisting of the rubidium and cesium salts of *meta*-substituted benzoates, respectively, follow the same trend as the second and third group: the melting and clearing points decrease with increasing size of the halogen substituent. However, the mesophase range decreases with increasing size for the rubidium salts, whereas the opposite was true for the sodium and potassium salts. Neither unsubstituted rubidium benzoate nor rubidium 3-fluorobenzoate show mesomorphism. Neither do any of the cesium salts. The thermal data of the rubidium and cesium salts of *meta*-substituted benzoates are given in Table 4 and 5, respectively.

Table 4. Thermal behaviour of *meta*-substituted rubidium benzoates

Compound	Transition temperatures (°C) <sup>[a]</sup>
Rubidium benzoate	Cr·444·I
Rubidium 3-fluorobenzoate	Cr <sub>I</sub> ·268·Cr <sub>II</sub> ·369·I
Rubidium 3-chlorobenzoate	Cr·308·SmA·334·I
Rubidium 3-bromobenzoate	Cr·260·SmA·279·I
Rubidium 3-iodobenzoate	Cr·232·SmA·244·I
Rubidium 3-methylbenzoate	Cr <sub>I</sub> ·248·Cr <sub>II</sub> ·299·SmA·375·I
Rubidium 3-methoxybenzoate	Cr <sub>I</sub> ·150·Cr <sub>II</sub> ·232·SmA·251·I

<sup>[a]</sup> Cr, Cr<sub>I</sub>, Cr<sub>II</sub>: solid crystalline phases; SmA: smectic A phase; I: isotropic phase.

Table 5. Thermal behaviour of *meta*-substituted cesium benzoates

Compound	Transition temperatures (°C) <sup>[a]</sup>
Cesium benzoate	Cr <sub>I</sub> ·383·Cr <sub>II</sub> ·398·I
Cesium 3-fluorobenzoate	Cr <sub>I</sub> ·256·Cr <sub>II</sub> ·303·I
Cesium 3-chlorobenzoate	Cr <sub>I</sub> ·218·Cr <sub>II</sub> ·288·I
Cesium 3-bromobenzoate	Cr <sub>I</sub> ·240·Cr <sub>II</sub> ·268·I
Cesium 3-iodobenzoate	Cr <sub>I</sub> ·221·Cr <sub>II</sub> ·235·I
Cesium 3-methylbenzoate	Cr <sub>I</sub> ·200·Cr <sub>II</sub> ·331·I
Cesium 3-methoxybenzoate	Cr <sub>I</sub> ·170·Cr <sub>II</sub> ·239·I

<sup>[a]</sup> Cr, Cr<sub>I</sub>, Cr<sub>II</sub>: solid crystalline phases; I: isotropic phase.

A sixth group of compounds comprises the lithium salts of the *meta*-substituted benzoates. The reason why they have not been discussed first is the aberrant behaviour of lithium in the alkali-metal series. The lithium–oxygen bonds are less ionic than the metal–oxygen bonds of the other alkali-metal ions. As a result, the thermal data of the lithium series are not in line with the results of the other *meta*-substituted benzoate salts. The mesophase range of the corresponding *meta*-chlorobenzoate increases in the same way, from 0 °C for the cesium salt (which is non-mesomorphic) through 26 °C for the rubidium salt and 61 °C for the potassium salt to 71 °C for the sodium salt. Looking only at the ionic radius of the alkali-metal ion, one would expect an even wider mesophase range for the lithium salt. This is not the case: lithium 3-chlorobenzoate has a mesophase range of 64 °C. The mesophase of lithium 3-iodobenzoate could not be identified (although it is very likely a highly ordered smectic phase). No nice texture could be observed under the microscope for any of the synthesised compounds. A very viscous mesophase is formed upon cooling the isotropic liquid, with no easily recognisable features present. This viscous phase does not crystallise when cooling further. This behaviour was observed in the DSC thermogram by the absence of a crystallisation peak in the first cooling run and a “cold” recrystallisation peak in the second heating run. The thermal behaviour of the lithium *meta*-substituted benzoates is summarised in Table 6.

Table 6. Thermal behaviour of *meta*-substituted lithium benzoates

Compound	Transition temperatures (°C) <sup>[a]</sup>
Lithium benzoate	Cr·369·I
Lithium 3-fluorobenzoate	Cr·310·SmA·340·I
Lithium 3-chlorobenzoate	Cr <sub>I</sub> ·186·Cr <sub>II</sub> ·284·SmA·348·I
Lithium 3-bromobenzoate	Cr·284·SmA·338·I
Lithium 3-iodobenzoate	Cr <sub>I</sub> ·197·Cr <sub>II</sub> ·265·M·333·I
Lithium 3-methylbenzoate	Cr·271·I

<sup>[a]</sup> Cr, Cr<sub>I</sub>, Cr<sub>II</sub>: solid crystalline phases; SmA: smectic A phase; M: unidentified smectic mesophase; I: isotropic phase.

The *ortho*- and *para*-substituted benzoates have also been studied. None of the *ortho*- (or 2-) or *para*- (or 4-)substituted benzoates shows mesomorphism. They all melt directly from the solid crystalline state to the isotropic liquid state. The melting points of the *para*-substituted salts are



higher than those of the *ortho*-substituted salts. Within the series of the *ortho*-substituted salts, the melting points decrease with increasing size of the halogen substituent. The same is true for the *para*-substituted series, although here the melting points of the 4-chloro-, 4-bromo- and 4-iodobenzoates are virtually the same. The thermal data for these compounds are collected in Table 7.

Table 7. Thermal behaviour of *ortho*- and *para*-substituted sodium benzoates

Compound	Transition temperatures (°C) <sup>[a]</sup>
Sodium benzoate	Cr·431·SmA·451·I
Sodium 2-fluorobenzoate	Cr·350·I
Sodium 2-chlorobenzoate	Cr·270·I
Sodium 2-bromobenzoate	Cr·260·I
Sodium 2-iodobenzoate	Cr·250·I
Sodium 4-fluorobenzoate	Cr·451·I
Sodium 4-chlorobenzoate	Cr·419·I
Sodium 4-bromobenzoate	Cr·420·I
Sodium 4-iodobenzoate	Cr·424·I

<sup>[a]</sup> Cr: solid crystalline phases; SmA: smectic A phase; I: isotropic phase.

The layer-like structure of the compounds in the smectic A phase indicates that a layer structure is also present in the solid state, as it is very unlikely that a layered structure is formed upon melting of these compounds. In the absence of a layered structure in the solid phase, the compound will directly melt to an isotropic liquid. Surprisingly few crystal-structure data of alkali-metal benzoates are available, and most of the structures described in the literature are those of acid salts (obtained by partial neutralisation of 1 mol of the benzoic acid with 0.5 mol of alkali-metal hydroxide).<sup>[12,13]</sup> To the best of our knowledge, only one crystal structure of an anhydrous alkali-metal benzoate is known: anhydrous lithium benzoate.<sup>[14]</sup> The lithium benzoate molecules form a two-dimensional structure consisting of a grid of lithium and carboxylate oxygen atoms, with the phenyl groups forming a covering layer on each side. The polymeric layers are stacked, with the CH groups in the *para*-position pointing towards each other, so that a bilayer structure is formed. The layers are held together by weak van der Waals forces. The authors relate the presence of the weak van der Waals forces to the easy cleavability of the sheetlike crystals.

The thermal behaviour of the alkali-metal benzoates can be described as follows: at the melting point the van der Waals bonds between the phenyl rings are broken, so that the layers can move relative to one another. Hence, we observe a smectic A mesophase. Most probably, the ionic layer containing the alkali-metal ions is partially destroyed too, otherwise the viscosity of the mesophase would be much higher than what we observe. At the clearing point, the polymeric ionic layer is totally broken into pieces, so that an ionic melt is formed. The substituents in the *ortho*-, *meta*- or *para*-position will have an influence on the stacking of the molecules. This effect will be most pronounced for compounds with substituents in the *ortho*-position, and

less so for compounds with substituents in the *meta*-position and in the *para*-position.

Although we tried out different routes, we were not able to obtain the anhydrous alkali-metal benzoates as single crystals of a quality high enough for X-ray diffraction. When an organic solvent was chosen as the crystallisation solvent only a fine polycrystalline precipitate was formed. Crystallisation from an aqueous solution resulted either in the formation of hydrated salts or of acid salts. The fact that those acids salts are formed in water, even though we started from pure alkali-metal benzoates, can be rationalised from the fact that, in water, partial hydrolysis occurs and the carboxylate groups get protonated. Nevertheless, these hydrated salts and acid salts do show the presence of a layered structure in the solid phase.

Single crystal data were obtained for four compounds: Rb(C<sub>7</sub>H<sub>4</sub>ClO<sub>2</sub>)(C<sub>7</sub>H<sub>4</sub>ClO<sub>2</sub>H) (**1**), Na(C<sub>7</sub>H<sub>4</sub>IO<sub>2</sub>)(H<sub>2</sub>O) (**2**), K(C<sub>7</sub>H<sub>4</sub>ClO<sub>2</sub>)(C<sub>7</sub>H<sub>4</sub>ClO<sub>2</sub>H) (**3**) and Rb(C<sub>7</sub>H<sub>4</sub>BrO<sub>2</sub>)(C<sub>7</sub>H<sub>4</sub>BrO<sub>2</sub>H) (**4**). All these compounds are salts of *meta*-substituted benzoic acids. The crystal data of compounds **1–4** are summarised in Table 8. Compounds **1**, **3** and **4** crystallised in the space group *C2/c*, whereas compound **2** crystallised in *P* $\bar{1}$  with two extra water molecules in the asymmetric unit. Consequently, the crystal packing of compounds **1**, **3** and **4** is isotypic, whereas compound **2** is differently packed. For compounds **1**, **3** and **4** the *meta*-chloro/bromobenzoic acid residues are linked together by a short, strong hydrogen bond across a centre of symmetry. The atom H7 lies on a centre of symmetry and bridges O2 and O2' of two centrosymmetrical equivalent residues (see Figure 7). The distances for this hydrogen bond (O···H···O distance) are 2.448(2), 2.438(3) and 2.434(9) Å for compounds **1**, **3** and **4** respectively. A search of the CSD<sup>[15]</sup> for benzoic acid compounds that exhibit a strong hydrogen bond with the hydrogen atom on a centre of symmetry gave an average distance of 2.451 Å, with a range of 2.432–2.480 Å, for 12 structures. No such hydrogen bonds were found for compound **2** (see Figure 8). The dihedral angles between the plane formed by the atoms of the planar phenyl ring and the plane through the carboxylic group are 8.4(1), 7.9(2) and 8.4(4)° for compounds **1**, **3** and **4** respectively. For compound **2** the carboxylic groups lie nearly perfectly in the plane of their respective phenyl rings. The angles are 0.56(17) and 0.73(17)° respectively.

For compounds **1**, **3** and **4** the coordination sphere of the alkali-metal ions (potassium or rubidium) can be described by a distorted octahedron. Each alkali-metal ion is surrounded by six carboxylate oxygen atoms from different benzoic acid residues. These six oxygen atoms actually consist of four O1 and two O2 atoms. Thus, every carboxylic O1 atom coordinates to two alkali-metal ions and every O2 atom to only one alkali-metal ion. The alkali metal–oxygen distances vary for the rubidium compounds in the range of 2.838(2)–3.043(2) and 2.845(7)–3.068(7) Å for compounds **1** and **4**, respectively, and for the potassium compound **3** from 2.724(4)–2.885(3) Å. Notice that the distances of the latter are a little shorter than for the rubidium compounds due to the smaller ionic radius. For compound **2** the asym-

Table 8. Summary of crystal data, intensity measurements, and structure refinement for compounds **1–4**

	1	2	3	4
Empirical formula	Rb(C <sub>7</sub> H <sub>4</sub> ClO <sub>2</sub> )-(C <sub>7</sub> H <sub>4</sub> ClO <sub>2</sub> H)	Na(C <sub>7</sub> H <sub>4</sub> IO <sub>2</sub> )-(H <sub>2</sub> O)	K(C <sub>7</sub> H <sub>4</sub> ClO <sub>2</sub> )-(C <sub>7</sub> H <sub>5</sub> ClO <sub>2</sub> H)	Rb(C <sub>7</sub> H <sub>4</sub> BrO <sub>2</sub> )-(C <sub>7</sub> H <sub>4</sub> BrO <sub>2</sub> H)
Formula mass	397.58	571.98	351.21	486.48
Dimensions (mm)	0.15 × 0.15 × 0.1	0.2 × 0.1 × 0.05	0.5 × 0.2 × 0.1	0.2 × 0.1 × 0.1
Crystal system	monoclinic	triclinic	monoclinic	monoclinic
Space group	<i>C</i> 2/ <i>c</i>	<i>P</i> $\bar{1}$	<i>C</i> 2/ <i>c</i>	<i>C</i> 2/ <i>c</i>
<i>a</i> (Å)	32.1084(12)	6.8673(3)	32.448(2)	32.889(2)
<i>b</i> (Å)	3.8104(10)	7.0112(3)	3.7577(3)	3.8563(3)
<i>c</i> (Å)	11.6212(4)	18.4121(7)	11.4010(8)	11.6525(8)
<i>a</i> (°)	90	84.104(3)	90	90
<i>β</i> (°)	96.446(2)	82.745(3)	94.631(4)	95.976(4)
<i>γ</i> (°)	90	89.622(6)	90	90
<i>V</i> (Å <sup>3</sup> )	1413.82(8)	874.74(6)	1385.58(17)	1469.85(18)
<i>Z</i>	4	2	4	4
<i>D</i> <sub>calcd.</sub> (g cm <sup>−3</sup> )	1.869	2.172	1.684	2.198
2 $\theta$ <sub>max</sub> (°)	142.78	142.56	141.84	142.98
$\mu_{Cu-K\alpha}$ (mm <sup>−1</sup> )	8.426	28.984	7.033	11.125
<i>F</i> (000)	784	536	712	928
Measured reflections	2388	7854	4618	4171
Unique reflections	1354	3211	1313	1359
Observed reflections [ <i>F</i> <sub>o</sub> > 4 $\sigma$ ( <i>F</i> <sub>o</sub> )]	1293	2853	1073	942
Parameters refined	108	217	96	96
<i>R</i> <sub>1</sub>	0.0351	0.0424	0.0464	0.0536
<i>wR</i> <sub>2</sub> [ <sup>a</sup> ]	0.0854	0.1070	0.1094	0.1161
<i>R</i> <sub>1</sub> (all data)	0.0364	0.0457	0.0586	0.0795
<i>wR</i> <sub>2</sub> (all data)	0.0871	0.1096	0.1164	0.1258

[<sup>a</sup>] Weighting scheme as defined for compound **1**:  $w = 1/[\rho^2(F_o^2) + (0.0422P)^2 + 0.8172P]$ , where  $P = [(F_o^2 + 2F_c^2)/3]$ ; compound **2**:  $w = 1/[\rho^2(F_o^2) + (0.0711P)^2]$ , where  $P = [(F_o^2 + 2F_c^2)/3]$ ; compound **3**:  $w = 1/[\rho^2(F_o^2) + (0.0596P)^2]$ , where  $P = [(F_o^2 + 2F_c^2)/3]$ ; compound **4**:  $w = 1/[\rho^2(F_o^2) + (0.0353P)^2]$  where  $P = [(F_o^2 + 2F_c^2)/3]$ .

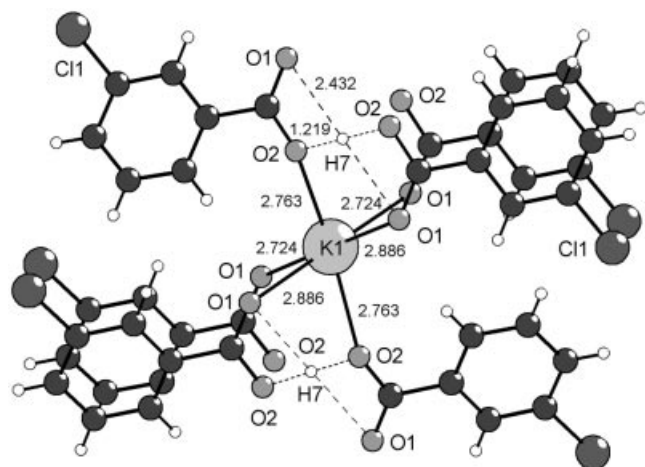


Figure 7. Crystal structure of compound **3** showing the coordination environment of the potassium ion; compounds **1** and **4** are isostructural

metric unit contains two alkali-metal (sodium) atoms. The coordination sphere of Na1 can be described by a distorted octahedron, which consists of six oxygen atoms, three from coordinated water molecules (O6 and two O5 atoms) and three from carboxylate oxygen atoms (O3, O2 and O4). The alkali metal–oxygen distances vary in the range 2.290(5)–2.609(5) Å. However, two additional longer contacts with O1 [2.903(6) Å] and O4' of another equivalent residue [2.995(5) Å] could be noticed. Na2 also exhibits an

octahedral coordination sphere, although it is less distorted than for Na1. The alkali metal–oxygen distances vary in the range 2.308(5)–2.831(5) Å with no additional contacts appearing. For compounds **1**, **3** and **4** the overall structure is built up by strands along the (010) direction, which are formed by the carboxyl O1 atom bridging the alkali-metal ions (see Figure 9). These strands are linked together in the (001) direction with the carboxylic groups acting as bridges (via O1) and with strong hydrogen-bonding between the O2 and O2' atoms of equivalent residues. As a result, a two-dimensional coordination polymer is formed. In the (100) direction only van der Waals forces are observed between these coordination polymer units: the shortest distance is between two Cl/Br atoms [3.503(3), 3.532(5) and 3.597(6) Å for compounds **1**, **3** and **4** respectively]. For compound **2**, however, a strand of sodium atoms is formed by the carboxylic O2 and O4 atoms, which bridge Na1 and Na2 along the (010) direction (see Figure 10). The carboxylic O1 and O3 atoms form additional contacts with Na1. Thus, in the (010) direction two different carboxylic groups bridge two strands of sodium ions. These double strands of sodium ions are linked together in the (100) direction by water molecules (O5 and O6), each contacting Na1 and Na2, which results in a two-dimensional coordination polymer. In the (001) direction no contacts other than van der Waals contacts could be observed; the shortest distance between two iodine atoms is 4.158(5) Å. The position of the benzoic acid substituent does not influence the overall crystal packing.

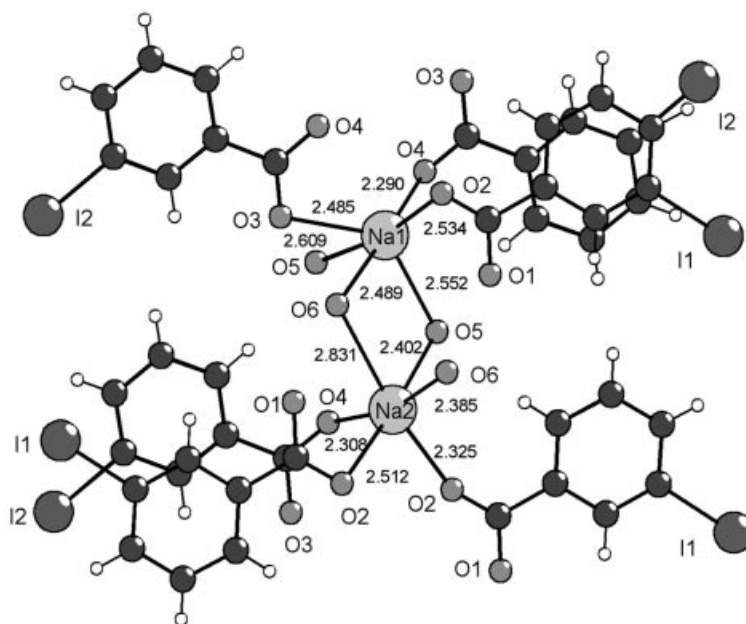


Figure 8. Crystal structure of compound **2** showing the coordination environment of the sodium ions

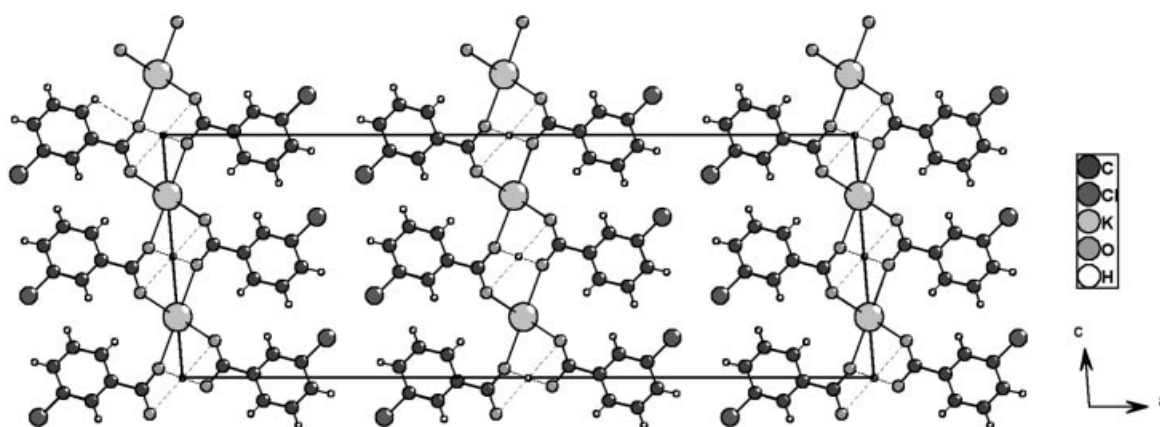


Figure 9. Crystal packing of compounds **1**, **3** and **4**

Indeed, for CSD<sup>[15]</sup> entry BINZAZ,<sup>[16]</sup> with a fluorine atom in the *para*-position, and for KHPHBZ10,<sup>[17]</sup> with a hydroxyl group in the *para*-position, a similar packing is observed. The latter crystallises in *P2/c* instead of *C2/c* (the *a*-axis is reduced to half length resulting in a similar packing) and contains one water molecule not in contact with the alkali-metal ion. Water molecules in contact with the alkali-metal ion influence the packing, as in compound **3**. The layered structures found for compounds **1–4** give an indication that it is likely that the anhydrous alkali-metal salts also have a layerlike structure in their solid phase. This idea is also supported by the fact that a layerlike structure is observed for lithium benzoate.<sup>[14]</sup> On the other hand, no layer structure is observed for benzoic acid. This compound forms dimers by intramolecular hydrogen bonding.<sup>[18]</sup> These dimers are not packed into layers, but are stacked on each other. The structure as a whole is built up by such stackings which alternate perpendicularly to one another. When the crystal melts, each dimer behaves as a separate

entity, but its length-to-width ratio is too small to form a mesophase. Therefore, benzoic acid and the substituted benzoic acids melt directly to the isotropic liquid without passing through a mesophase.

Due to the absence of alkyl chains, the transition temperatures of the compounds are very high. At these high temperatures, the thermal energy of the molecules is high as well and only compounds with a strong interaction between the metal and carboxylate groups will exhibit a mesophase. Based on the concept of the hardness of Lewis acids and Lewis bases,<sup>[19]</sup> the strength of the metal–carboxylate bond decreases in the order  $\text{Na}^+ > \text{K}^+ > \text{Rb}^+ > \text{Cs}^+$ . Therefore, sodium compounds have the highest tendency to form a mesophase. This is indeed observed experimentally. The high transition temperatures result in several compounds starting to decompose in the mesophase (or even before the mesophase is reached). Lithium compounds are an exception, because the lithium–oxygen bond has a higher covalent contribution than the same bond in the



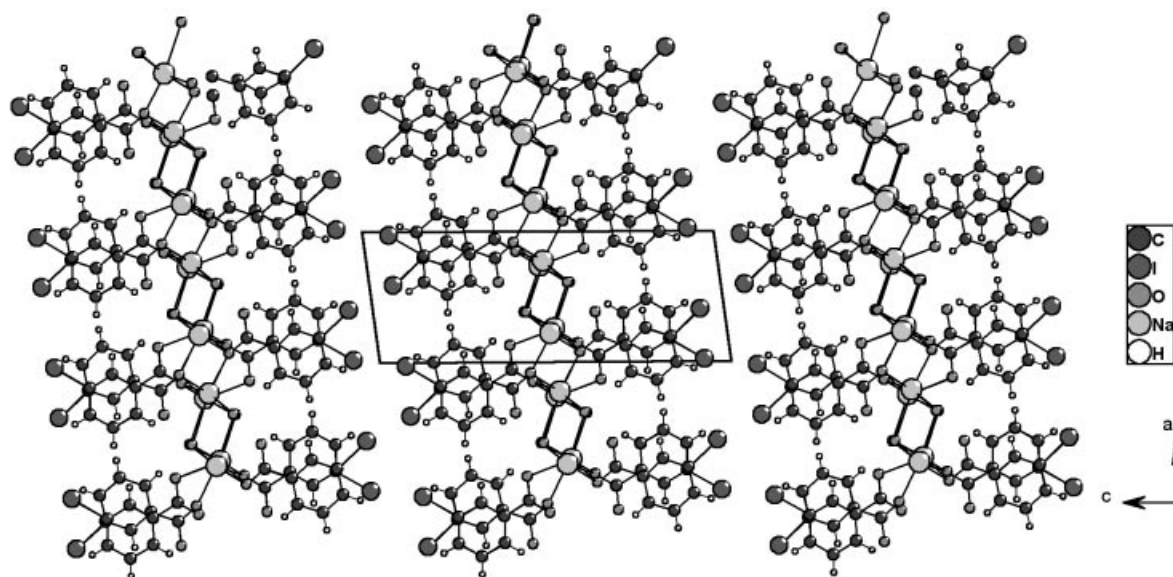


Figure 10. Crystal packing of compound 2

other alkali metals. The higher the transition temperatures, the higher the chance that the compounds will melt from the solid state directly to the isotropic liquid. This is especially true when the strength of the ionic layer is weakened by (bulky) substituents in the *ortho*-position of the benzene ring. Bulky groups in the *para*-position prevent the formation of a mesophase, because the molecules will experience larger van der Waals forces or even dipole–dipole interactions, and because the bulky groups make it more difficult for the layers to glide along one another (and thus also give a higher viscosity). From this viewpoint, it is understandable that the most stable mesophases are formed for the alkali-metal salts of the *meta*-substituted benzoic acids. No mesophase is expected for the alkali-metal salts of terephthalic acid, because in this case no layer structure with an alternation of layers with ionic and van der Waals forces will be formed, but a succession of ionic layers.

## Conclusion

Although the alkali-metal salts of aromatic carboxylic acids don't have the rodlike or disklike shape of conventional liquid crystals, they can form a mesophase at high temperatures. This has been illustrated for the salts of different substituted benzoic acids. The position of the substituent is of prime importance, since only the salts of *meta*-substituted benzoic acids exhibit mesomorphism. No liquid-crystalline behaviour was observed for *ortho*- and *para*-substituted compounds. The mesomorphism not only depends on the type of substituent and its position, but also on the type of alkali metal. The most stable mesophases were observed for the sodium salts, and of the salts of unsubstituted benzoic acid, only sodium benzoate is mesomorphic. Investigation by polarizing optical microscopy and by high-temperature X-ray diffraction shows that the structure of the mesophase is similar to that of the smectic A phase of conventional

organic liquid crystals. Crystal structures of similar, but hydrated or solvated compounds show that a layer-like structure is already present in the solid state.

## Experimental Section

The alkali-metal salts were prepared by a neutralisation titration of an ethanolic solution of the carboxylic acid with an aqueous standard solution (0.5 M) of the corresponding alkali-metal hydroxide (LiOH, NaOH, KOH, CsOH or RbOH), with phenolphthalein as the indicator. After reaching the equivalence point, the carboxylate salts were recovered by evaporation of the solvent under reduced pressure. The compounds were redissolved in a small amount of ethanol at room temperature and were reprecipitated by addition of acetone or a mixture of acetone and diethyl ether. An acetone/diethyl ether mixture was used for the precipitation of the rubidium and the cesium salts of sodium 2-chlorobenzoate and sodium 2-bromobenzoate. The precipitate was filtered off on a Buchner funnel, washed with acetone and dried *in vacuo* at 120 °C. The purity of the samples could not be checked by CHN elemental analysis, because the carbon dioxide, resulting from the combustion of the benzoic acids in the CHN apparatus, reacts with the alkali metals to form alkali-metal carbonates, which are very stable at high temperatures, resulting in a too low measured carbon content. All samples were prepared in triplicate to check the reproducibility of the transition temperatures. Infrared measurements were performed to check the absence of free carboxylic acid.

Differential scanning calorimetry (DSC) measurements were performed on a Mettler-Toledo DSC821e module (scan rate 10 °C min<sup>-1</sup> under a helium flow of 35 mL min<sup>-1</sup>). The reported transition temperatures are onset temperatures. The optical textures of the mesophases were observed with an Olympus BX60 polarizing optical microscope equipped with a Linkam THMS600 hot stage and a Linkam TMS93 programmable temperature controller. In order to avoid or reduce the oxidative degradation of the compounds, the hot stage was flushed with a stream of nitrogen gas. High-temperature X-ray diffraction was measured on a STOE Transmission Powder Diffractometer System STADI P, with a high temperature attachment version 0.65.1 (temperature range from



room temperature to 1000 °C). Monochromatic Cu- $K_{\alpha 1}$  radiation ( $\lambda = 1.5406 \text{ \AA}$ ) was obtained with the aid of a curved germanium primary monochromator. The diffracted X-rays were measured by a linear Position Sensitive Detector (PSD). The sample was placed in a quartz glass capillary (outer diameter 0.3 mm, wall thickness 0.01 mm) and spun during the measurement.

Crystals of salts of the *meta*-substituted benzoates of a quality suitable for X-ray diffraction were obtained for Rb(C<sub>7</sub>H<sub>4</sub>ClO<sub>2</sub>)(C<sub>7</sub>H<sub>4</sub>-ClO<sub>2</sub>H) (**1**), Na(C<sub>7</sub>H<sub>4</sub>IO<sub>2</sub>)(H<sub>2</sub>O) (**2**), K(C<sub>7</sub>H<sub>4</sub>ClO<sub>2</sub>)(C<sub>7</sub>H<sub>4</sub>ClO<sub>2</sub>H) (**3**) and Rb(C<sub>7</sub>H<sub>4</sub>BrO<sub>2</sub>)(C<sub>7</sub>H<sub>4</sub>BrO<sub>2</sub>H) (**4**) by slow evaporation of the solvent from an H<sub>2</sub>O/EtOH (1:1) mixture at room temperature, and mounted in a nylon loop for data collection at 100 K on a SMART 6000 diffractometer equipped with a CCD detector using Cu- $K_{\alpha}$  radiation ( $\lambda = 1.54178 \text{ \AA}$ ). The images were interpreted and integrated with the program SAINT from Bruker.<sup>[20]</sup> The four structures were solved by direct methods and refined by full-matrix least-squares on  $F^2$  using the SHELXTL program package.<sup>[21]</sup> Non-hydrogen atoms were refined anisotropically and the hydrogen atoms were refined in the riding mode with isotropic temperature factors fixed at 1.2-times  $U(\text{eq})$  of the parent atoms, except for compound **1**, where the positions of all hydrogen atoms could be localised from the difference Fourier maps without applying any further restraints. For compounds **1**, **3** and **4** the H atoms occur on special positions — the H7 atom bridges O2 and O2' of a symmetry-equivalent molecule. Only for compound **4** could this H atom not be localised from the difference Fourier maps; it was modelled by assigning the coordinates of the special position. Compound **3** is essentially the same as the one found in the CSD<sup>[15]</sup> with code KHCBZO10,<sup>[12]</sup> but in the latter one aromatic hydrogen atom and the one at the special position are not included in the structure.

CCDC-256797 (**1**), -256798 (**2**), -256799 (**3**) and -256800 (**4**) contain the supplementary crystallographic data for this paper. These data can be obtained free of charge at [www.ccdc.cam.ac.uk/conts/retrieving.html](http://www.ccdc.cam.ac.uk/conts/retrieving.html) [or from the Cambridge Crystallographic Data Centre, 12 Union Road, Cambridge CB2 1EZ, UK; Fax: + 44-1223-336-033; E-mail: [deposit@ccdc.co.uk](mailto:deposit@ccdc.co.uk)].

## Acknowledgments

K. B. and R. V. D. thank the F.W.O.-Flanders (Belgium) for a Post-doctoral Fellowship. Financial support by the F.W.O.-Flanders

(G.0117.03) and by the K.U.Leuven (GOA 03/03) is gratefully acknowledged. The authors thank Prof. Gerd Meyer and Dr. Dirk Hinz-Hübner (University of Cologne, Germany) for access to XRD facilities and for measurements of X-ray diffractograms, respectively.

- [1] C. Tschierske, *J. Mater. Chem.* **1998**, 8, 1485–1508.
- [2] *Handbook of Liquid Crystals*, vols. I and IIB (Eds.: D. Demus, J. Goodby, G. W. Gray, H.-W. Spiess, V. Vill, Wiley-VCH, Weinheim, **1998**.
- [3] D. Vorländer, *Z. Physik. Chem.* **1927**, 126, 449–472.
- [4] P. A. Irvine, D. C. Wu, P. J. Flory, *J. Chem. Soc., Faraday Trans. 1* **1984**, 80, 1795–1807.
- [5] I. C. Lewis, C. A. Kovac, *Mol. Cryst. Liq. Cryst.* **1979**, 51, 173–178.
- [6] T. J. Dingemans, N. S. Murthy, E. T. Samulski, *J. Phys. Chem. B* **2001**, 105, 8845–8860.
- [7] M. Kölb, T. Beyersdorff, C. Tschierske, S. Diele, J. Kain, *Chem. Eur. J.* **2000**, 6, 3821–3837.
- [8] J. Barbera, O. A. Rakitin, M. B. Ros, T. Torroba, *Angew. Chem. Int. Ed.* **1998**, 37, 296–299.
- [9] D. Vorländer, *Ber. Dtsch. Chem. Ges.* **1910**, 43, 3120–3135.
- [10] D. W. Bruce, K. Heyns, V. Vill, *Liq. Cryst.* **1997**, 23, 813–819.
- [11] D. Demus, H. Sackmann, K. Seibert, *Wiss. Z. Univ. Halle* **1970**, 19, 47–62; *Chem. Abstr.* **1971**, 75, 123351w.
- [12] A. L. Macdonald, J. C. Speakman, *J. Chem. Soc., Perkin Trans. 2* **1972**, 1564–1566.
- [13] H. N. Shrivastava, J. C. Speakman, *J. Chem. Soc.* **1961**, 1151–1163.
- [14] D. A. Plattner, W. Petter, D. Seebach, *Chimia* **1994**, 48, 138–141.
- [15] F. H. Allen, *Acta Crystallogr., Sect. B* **2002**, 58, 380–388.
- [16] J. Longo, M. F. Richardson, *Acta Crystallogr., Sect. B* **1982**, 38, 2482–2483.
- [17] L. Manojlovic, *Acta Crystallogr., Sect. B* **1968**, 24, 326–330.
- [18] R. Feld, M. S. Lehmann, *Z. Kristallogr.* **1981**, 157, 215–231.
- [19] R. G. Pearson, *J. Am. Chem. Soc.* **1963**, 85, 3533–3539.
- [20] SAINT, Manual Version 5/6.0, Bruker Analytical X-ray Systems Inc., Madison, Wisconsin, **1997**.
- [21] SHELXTL-NT, Manual Version 5.1, Bruker Analytical X-ray Systems Inc., Madison, Wisconsin, **1997**.

Received May 13, 2004

Early View Article

Published Online December 13, 2004